Numerical Comparison of an Ethanol Spray Using Open FOAM and Star CCM+

Roberto Ribeiro Schor

Leonardo Mayer Reis

Marilia Gabriela Justino Vaz

Deborah Domingos da Rocha

Rudolf Huebner

Ramon Molina Valle

roberto.schor@gmail.com

leo1mayer@gmail.com

mariliagabrielavaz@hotmail.com

debyddr@gmail.com

rudolf@demec.ufmg.br

ramon@demec.ufmg.br

Universidade Federal de Minas Gerais

Av. Pres. Antnio Carlos, 31270-901, Minas Gerais, Belo Horizonte, Brazil

Abstract. *Internal combustion engines are thermal machines that convert chemical energy from fuels into mechanical energy through combustion. Stringent regulations regarding the emission of pollutants demand the development of advanced combustion technologies. The Direct Injection (DI) of fuel into the combustion chamber of a Spark Ignition (SI) engine is a strategy that is widely recognized for having the potential to improve fuel efficiency. In addition, the search of biofuels, such as Ethanol, is an option to reduce the pollution and environmental impacts. The development of an optimized combustion for Ethanol DI engines require a very accurate formation of an ignitable fuel-air ratio, which is a process that begins with the proper injection of fuel. CFD simulations are widely used to analyze the formation of a fuel spray in the cylinder of the engine. Although several mature commercial CFD packages are on the market, there is also the need for a less expensive software. Therefore, there is a growing interest in some software such as OpenFOAM. In this paper it is going to be compared a simulation of a spray produced by a pressure-swirl injector into a static chamber at atmospheric pressure using the commercial*

software Star-CCM+ with a simulation of the same process but using the open source software OpenFOAM.

Keywords: *OpenFOAM, Star CCM+, KHRT, Reitz-Diwakar, CFD*

1 INTRODUCTION

The growth in global energy consumption is causing several environmental issues. The transport sector consume around 55% of global oil resources and produce around 25% of the global greenhouse gas (Huang, 2014). Light-duty vehicles, such as passenger cars, account for a large proportion of the transport sector oil consumption. Emissions from passengers cars includes carbon monoxide (CO), hydrocarbons (HC), nitrogen oxides (NO_x) and particulate matter (PM) are harmful to both the environment and human health. With this in mind the EU proposed an regulation to reduce these types of emissions from Light-duty vehicles, in Fig. 1 it is shown how the emissions of CO_2 will be regulated in the near future.

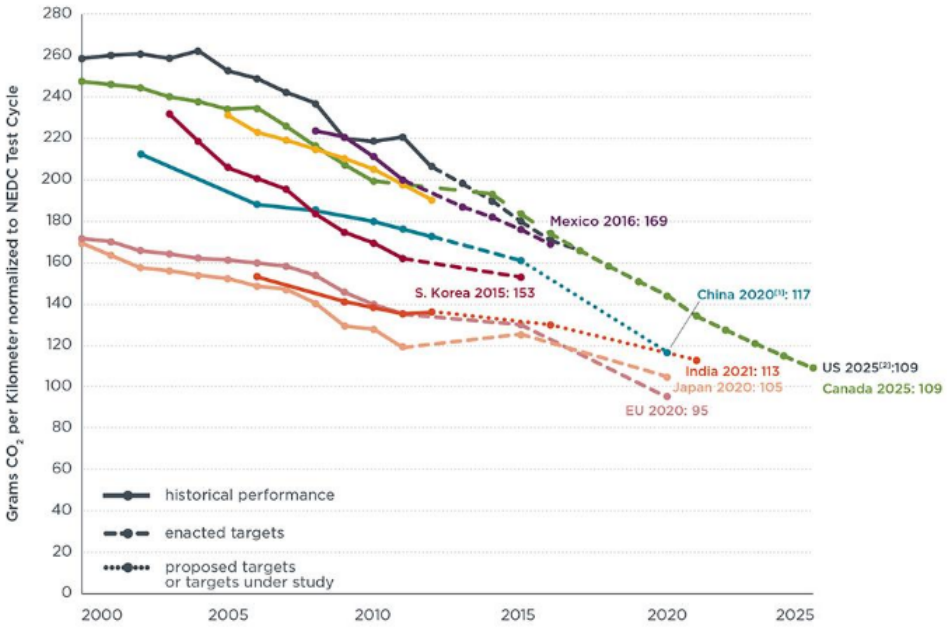

Figure 1: Comparison of historical and target Light Duty Vehicle CO2 emission rates (Huang, 2014)

Other countries such as Brazil and the US have also imposed regulations regarding emissions. In Brazil, PROCONVE Emission Standards for Passenger Vehicles imposed that from 2014 forward the CO, NO_x and PM emissions could not surpass 2.0[g/Km],0.08[g/Km] and 0.025[g/Km], respectively (DieselNet, 2017).

To satisfy this stringent requirements for ultra-low emission and highly efficient energy production, it has become necessary the study of technologies to reduce fuel consumption and to decrease emissions in Internal Combustion Engines.

Downsizing and downspeeding are exemples from technologies able to reduce engine size and maintain the power and torque of it. To do so it is imperative to study the effects of the Direct Injection mechanism.

The evolution of high-pressure-injection technology will result in fine atomization and will provide better air-fuel mixture (Lee, 2008). To optimize the injection into the cylinder, characteristics such as spray penetration, Sauter Mean Diameter (SMD) and fuel distribution need to be carefully studied.

Multidimensional models for computing fuel spray dynamics have been under development for more two decades. Among the models, the Lagrangian stochastic method has been

demonstrated to be computationally efficient and successful in ethanol spray predictions. This method solves the governing equations for the gas phase and the interactions between the liquid drops and the gas phase. To compute spray dynamics, discrete drops are introduced into the computation domain in the form of groups or parcels of particles, and each computational parcel represents a number of droplets of identical size, velocity, and temperature. The more points, the more accurate representation of the spray (Lucchini et al., 2005).

The Computational Fluid Dynamics, CFD, has developed to the point where the complete three dimensional flow field over the vehicle and through engines can be computed expeditiously with accuracy and reliability. To achieve this requirement, the industry must investigate a range of factors that can potentially reduce engine emissions, including fuels, combustion process, chemical-kinetics, in-cylinder flow, fuel-air mixture formation, sprays, engine geometries, etc. Nowadays, computational simulations have been adopted as a key analysis tool in engine research to establish correlation with experimental studies and provide new information for designers. A significant advantage of using CFD is the flexibility of simulation setups and the time and cost reduction compared to experiments. Major CFD commercial codes that are available in the market currently include Ansys CFX, Ansys Fluent, AVL Fire, CD-adapco Star-CD, Star-CCM+, on the other hand it is possible to use an open source code as the OpenFOAM.

Two software have been tested, OpenFOAM and StarCCM+. The computational model have been performed to study the atomization processes of hollow cone fuel sprays from a high pressure swirl injector for ethanol direct injection engines. The objective has been to obtain reliable comparison between the commercial software and the open source software. Computed and measured spray characteristics, such main-spray structure, tip penetration and break-up phenomena, have been compared, achieving good levels of agreement.

2 Spray numerical model

There are several methods to introduce particles in the system. In sprayFoam the particles are introduced through the injectors, in according to settings specified by the user. The simplest approach to modelling primary atomization involves seeding a number of different parcels at the position of the injector nozzle (Huang, 2014). Properties and behavior of all droplets in the spray can be approximately represented by these discrete droplets (Baumgarten, 2006). Nevertheless, in order to have the correct fuel mass in the cylinder, the mass of all droplets must be regarded. This is why every representative droplet gets a number of further droplets with identical size, temperature and velocity components etc., who have exactly the same behavior and properties like the representative one. These groups of equal droplets are called parcels.

In case of a hollow cone spray, an annular liquid sheet is produced at the nozzle orifice forming a free cone-shaped liquid sheet that disintegrates into droplets. There are several ways to describe the distribution of the particles during this stage, such as Rosin-Rammler distribution, Chi-square, the Exponential function and Linearized Instability Sheet Atomization (LISA).

The LISA model highlights the growth of perturbations on a liquid surface due to the Kelvin-Helmholtz instability as the driving force of primary atomization (Huang and Lipatnikov, 2011). The LISA model is divided into three stages: film formation, sheet breakup and atomization (Shim et al., 2008). Equation (1) shows the thickness from the film is related to the mass flow:

$$\dot{m} = \pi \rho u t (d_0 - t). \tag{1}$$

In Equation (1) the ρ is the density of the fuel injected, d_0 the Injector exit diameter (μm), t the film thickness at the injector exit (μm) and u the axial component of velocity determined by Equation (2) where is the angle of the spray.

$$u = U_i nj cos(\theta) \tag{2}$$

It is also assumed that the total injection velocity $U_i nj$ is the pressure difference between the injection pressure and the counter-pressure of the chamber, in other words, it is the absolute velocity of the sheet. It should be differentiated of the quantity U the relative velocity between liquid and gas.

$$U_i nj = k_v \sqrt{\frac{2\Delta p}{\rho_l}}. \tag{3}$$

$$k_v = \left[0.7, \frac{4\dot{m}}{\pi d_0^2 \rho_l \cos(\theta)} \sqrt{\frac{\rho_l}{2\Delta p}}\right]. \tag{4}$$

With Equation (3) and Equation (4) it is possible to determinate the total velocity in relation to the injector pressure, where ρ_l is the density of the liquid injected. The sheet will break up and ligaments will be formed at a length given by Equation (5).

$$L = U_i nj \tau = \frac{U}{\Omega} \ln \frac{\eta_b}{\eta_0} \tag{5}$$

Based on Dombrowski and Hooper work, the value of $\ln \frac{\eta_b}{\eta_0}$ is taken 12.

If it assumed that the ligaments are formed from tears in the sheet, once per wavelength, the resulting diameter is given by Equation (6) and the wave number of the fastest growing surface wave K_s by Equation (7).

$$d_L = \sqrt{\frac{16h}{K_s}}. \tag{6}$$

$$K_s = \frac{p_2 U^2}{2\sigma}. \tag{7}$$

Where p_2 is the pressure of the chamber and σ the superficial liquid tension.

Using the stability analysis, the disintegration of the ligament into drops is calculated. The breakup occurs when the amplitude of the unstable waves is equal to the radius of the ligament and that one droplet will be formed per wavelength. The diameter will be given by Equation (8) and Equation (9).

$$K_L d_L = \left[\frac{1}{2} + \frac{3\mu_l}{2(\rho_l \sigma d_L)^{\frac{1}{2}}}\right]^{\frac{1}{2}}. \tag{8}$$

$$d_D^3 = \frac{3\pi d_L^2}{K_L}. \tag{9}$$

Secondary breakup models are designed to simulate the formation of smaller droplets in the downstream of a spray. The secondary breakup can be approximated to a processes of continue reduction of the radius of the droplet, Equation (10), this is known as the Reitz-Diwakar model.

$$\frac{dr}{dt} = -\frac{r - r_{RD}}{\tau_{RD}} \tag{10}$$

The Equation (10) follows the empirical Equation (11) and Equation (12) when $We_g > 0.5\sqrt{Re_g}$, Equation (13) and Equation (14) when $6 < We_g < 0.5\sqrt{Re_g}$ and the droplet radius is assumed to be constant if $We_g < 6$.

$$\tau_{RD} = B_{RD}\frac{r}{U}\sqrt{\frac{\rho_f}{\rho_g}} \tag{11}$$

$$r_{RD} = \frac{\sigma^2}{2\rho_g U^3 \nu_g} \tag{12}$$

$$\tau_{RD} = \pi\sqrt{\frac{\rho_f r^3}{2\sigma}} \tag{13}$$

$$r_{RD} = \frac{6\sigma}{\rho_g U^2} \tag{14}$$

We and Re are the Weber and Reynolds number, respectively, both of which calculated for the gas phase. ρ is the density and σ is the surface tension coefficient of the fuel, ν is the kinematic viscosity, U is the magnitude of the gas velocity vector with respect to the droplet,

and the subscripts g and f designate the gas and liquid fuel, respectively. The default value of the constant B_{RD} is 20 (Huang, 2014).

Another model for the secondary breakup is the Kelvin-Helmholtz/Rayleigh-Taylor model (KHRT). The KHRT model considers droplet breakup to be caused by the growth of two instabilities, the KH instability addressed by the wave model and the RT instability developing on the droplet surface under the influence of the flow acceleration.

Limiting the case of negligible viscosity of the fluids, it is possible to derivative the equations for the wavenumber (K_{RT}) and growth rate (Ω_{RT}) (Bellman, R., Pennington, 1953).

$$K_{RT} = \sqrt{\frac{-a(\rho_f - \rho_g)}{3\sigma}} \tag{15}$$

$$\Omega_{RT} = \sqrt{\frac{2}{3\sqrt{3\sigma}} \frac{[-a(\rho_f - \rho_g]^{\frac{3}{2}}}{\rho_f + \rho_g}} \tag{16}$$

With ρ_g as the density of the cylinder gases and a as acceleration.

$$a = -\frac{3}{8} C_D \frac{\rho_g U^2}{\rho_f r} \tag{17}$$

Equation (17) relates the Drag Force, C_D , with the acceleration. Where r is the radio of the droplet.

Different methods were proposed to simulate the new radius.

For comparison purpose, some macroscopic characteristic of sprays has been studied as liquid length penetration, in order to correlate numerical and experimental data. The shadowgraph technique is an optical method for the flow visualization used in data acquisition. But, the frequency of this data is limited by the camera frame rate, this can be overcome by the numerical simulation.

The length penetration (S), as illustrated in Fig. 2, is define the maximum liquid length penetration at each time, limited by the distance between the nozzle and the piston. For the pressure-swirl spray, the pre-spray is not account in the calculation.

However, the experimental definition is based on a threshold value of light intensity and cannot be directly converted into exact percentage of liquid. Values such as 95, 97 and 99 percent of the liquid mass found on the farthest position of the injection point have been used as penetration definition.

Other of the microscopic characteristics of spray is the parameter that quantify the diameter of droplets. Then, there are many representative diameters that can be used, they are calculated based on the diameter and the frequency that these droplets appears on spray structure. One of the most used is called Sauter Mean Diameter (SMD), which represents a diameter of a droplet whose ratio of volume to surface area is representative as the entire spray at an specific

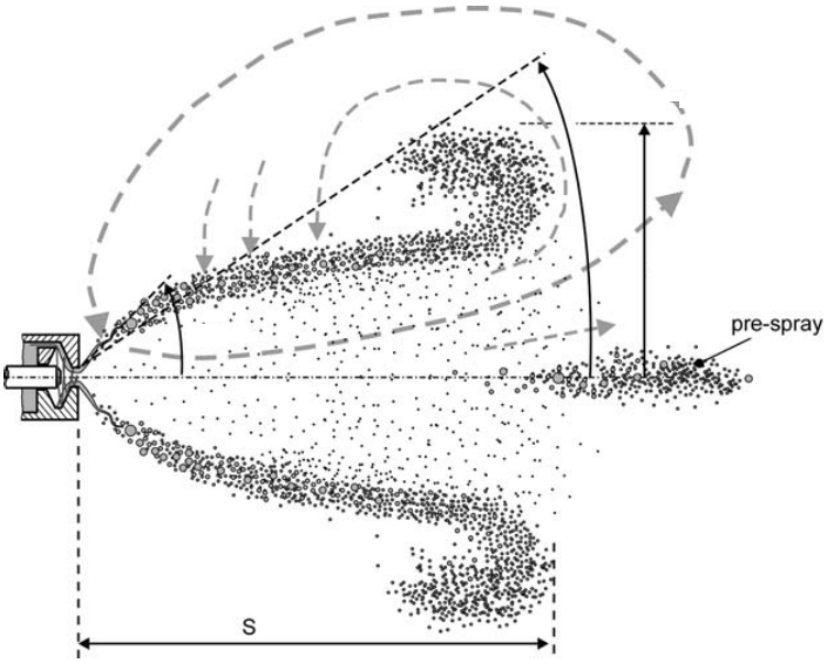

Figure 2: Typical spray from a pressure-swirl atomizer and the penatration definition (Baumgarten, 2006)

time (Lefebvre, 1989). The SMD is calculated as shown in Equation (18) where d_i is the droplet diameter and N_i is the number of droplet with this diameter.

$$SMD = \frac{\sum_{n=1}^{n} N_i (d_i)^3}{\sum_{n=1}^{n} N_i (d_i)^2} \tag{18}$$

2.1 Metodology

The injector used for this simulations is shown in Fig. 3. It is a direct injection, model IWD3 + 193 of Magneti Marelli. The boundary and initial conditions were collected during experimental test. This tests has been carried out with the aid of the high speed shooting and Shadowgrafia technique in Mobility Technology Center (CTM). This experimental data was used in all simulations.

Figure 3: Injector of Magneti Marelli (Guzzo, 2015)

The laboratory tests and processing of the images, in order to obtain the cone angles, border

format of the spray, the spray penetration, and others, are described in GUZZO [10,11]. Table 1 shows the boundary and initial conditions for the injector.

Table 1: Initial and Boundary conditions for the injector

Boundary Parameter	Unity	Value
Chamber Temperature	K	300
Chamber Presure	kPa	100
Injection Temperature	K	320
Injection Pressure	kPa	10000
Inner Cone Angle	$^{\circ}$	40
Outer Cone Angle	$^{\circ}$	69.1
Mean Mass Flux	g/s	12.65
Injection Pressure	kPa	10000
Injector Position (x,y,z)	m	(0 ; 0 ; 0.12)
Injector Direction (x,y,z)	m	(0.00209 ; 0 ; 0.9999)

There is no consensus in the literature about the number of parcels injected per time step in the attempt to adequately represent the spray. In this work, it is proposed to insert in the computational domain 300 parcels at the end of each time step. The total injection time was defined as 1.5 ms based on the experiment test parameter.

The fuel used in the simulations was Ethanol (C2H5OH). The properties used in STAR-CCM + 9 software are those corresponding to the literature [12,13,14]. The properties are listed in Table 2.

Table 2: Properties of Ethanol

Properties	Unity	Value
Density	kg/m^3	784.885
Dynamic Viscosity	$Pa * s$	0.00108407
Lower Heating Value	J/kg	-5998370
Saturation Pressure	Pa	7871.66
Specific Heat	$J/kg * K$	2434.31
Surface Tension	N/m	0.0223

When utilizing the OpenFOAM software, it was used the NSRDS functions to calculate the requested properties for a specific pressure and temperature. But the base propretie was the same as the STAR-CCM + 9.

2.2 Star-CCM+

The experimental domain used was cylindrical prism with 100 mm height and 70 mm diameter (Fig. 4).Therefore, numerical domain used was a cylindrical chamber of 100 mm height and 70 mm diameter (Fig. 4), as the experimental test chamber. The simulations were based on spray penetration experiment in order to avoid the contact with the walls of the physical domain.

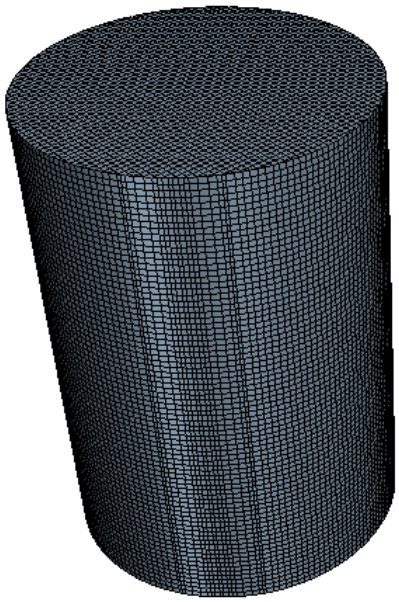

Figure 4: Numerical Domain of the Spray in Star-CCM+

All regions of the cylindrical chamber were treated as wall regions with a temperature of 300 K. The software requires the insertion of a turbulent intensity and an initial turbulent viscosity rate were set at 0.01 and 0.1 respectively (CD-ADAPCO, 2014) . According to the literature, the CFD simulations for injections spray results are sensitive to the mesh (Baumgarten, 2006). Based on previous studies (Park et al., 2009), to assess the dependence of the mesh were made five distinct meshes with an average size of elements of 0,75; 1; 1.25; 1.5; 1.75; 2 mm. All meshes were simulated with the step time of $5\text{x}10^{-6}s$. It were used 100 iterations for each time step. The mesh 0.75mm presented the best results and it was used in all Star-CCM+ simulations.

The LISA model was the primary break-up model used in these simulations. However, for the the secondary break-up two different models were used: Reitz Diwakar and KHRT. According to the literature (Kah et al., 2012), it is suggested for the best results, that the two constants of KHRT model can be altered : B1=8 and C3=C_{tau}= 2 for the Ethanol fuel injection. These parameters was adopted in all simulations. The table 3 resume the Star-CCM+ simulations.

2.3 OpenFOAM

The numerical domain was specified to be a rectangular prism with the dimension 40x100x40 mm with the average cell size of 1mm (Fig. 5).

Table 3: Star-CCM+ simulations

Simulation	Primary Break-up	Secondary Break-up	Software
S1	LISA	Reitz Diwakar	Star-CCM+
S2	LISA	KHRT	Star-CCM+

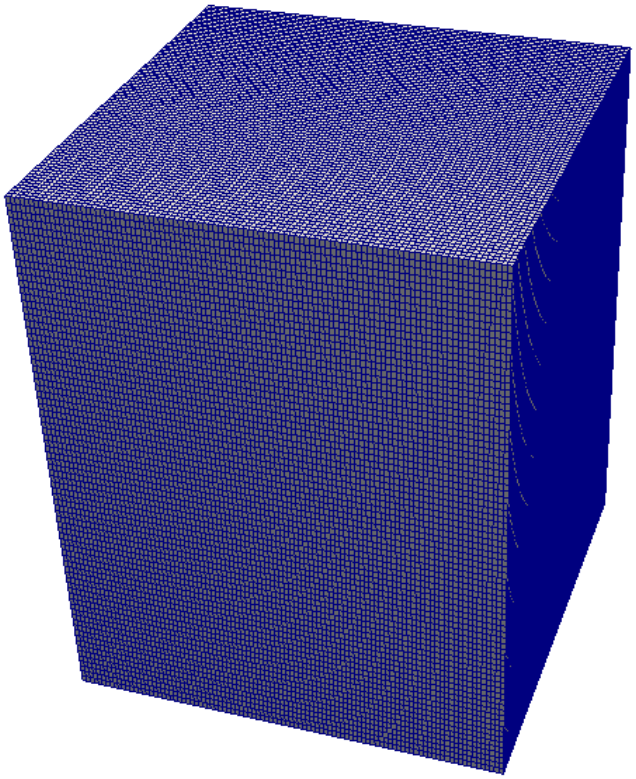

Figure 5: Numerical Domain of the Spray in OpenFOA

This prism contains 656100 hexahedral and no non-orthogonality. Another detail that was addressed is that the direction of the spray is aligned with the mesh. Within the description of the problem it is defined the inner and outer angle of the hollow cone spray. The parcels are randomly and uniformly distributed between this angle. The total inject fuel, injection temperature and injection pressure are also defined in this step. As in the Star-CCM +, the two types of secondary break-up were used. The simulations are summarized in Table 4.

Table 4: OpenFOAM simulations

Simulation	Primary Break-up	Secondary Break-up	Software
S3	LISA	Reitz Diwakar	OpenFOAM
S4	LISA	KHRT	OpenFOAM

It is important to point out that the collision model was not used, neither for Star-CCM+ nor OpenFOAM.

2.4 Results and Discussions

Penetration

The penetration curves obtained for these simulations were compared with the experimental data with their respective upper and lower limits. These results are shown in Fig. 6 and Fig. 7.

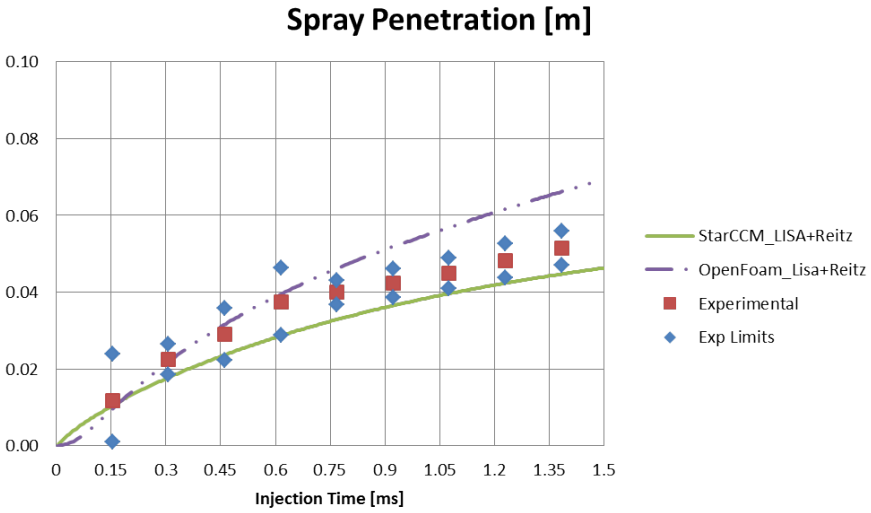

Figure 6: Penetration for the Reitz Diwakar model simulations

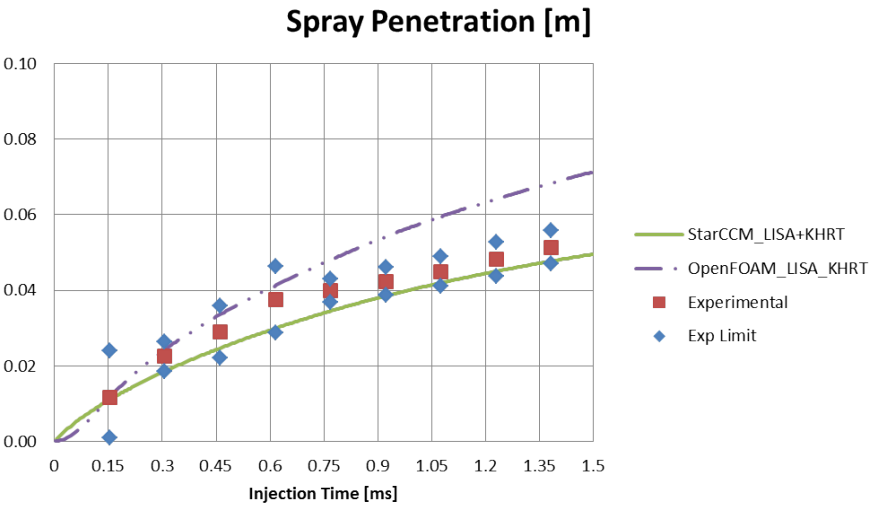

Figure 7: Penetration for the KHRT model simulations

It is possible to note similar behavior of the four simulations to the experimental average data in the beginning of the injection, until 0.7ms, as observed in Fig. 6 and Fig. 7. It is important to note that the methodology used in numerical models do not consider the pre-spray, in Fig. 8 one can see the initial pre-spray side by side with both models utilized in OpenFOAM.

It is also important to observe that the Star CCM + (Version 9) Rate Of Injection (ROI) is constant and equal to 12.65 g/s and that for the OpenFOAM simulations it was implemented a

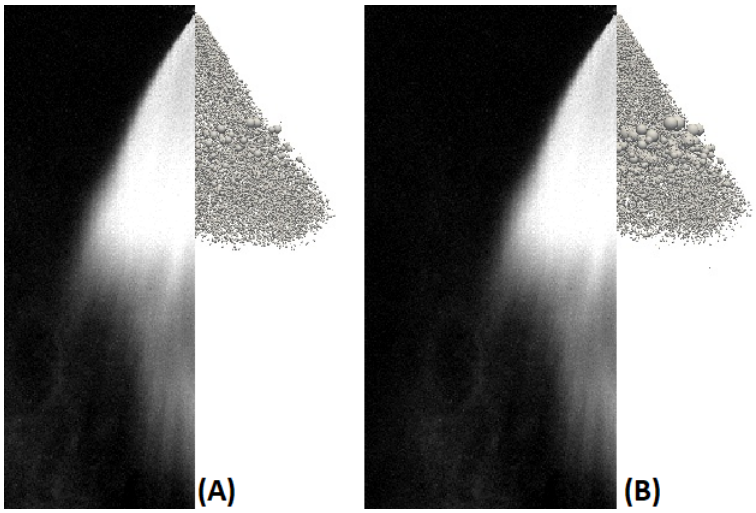

Figure 8: OpenFOAM: (A) - Images of Reitz Diwakat model / (B) - Images KHRT at 0.6ms

trapezoidal ROI. This difference is possible to observe in the initial 0.15ms in Fig. 6 and Fig. 7. With the trapezoidal injection there is an inflection on the penetration curve, on the contrary with the constant ROI there isn't an inflection in the curve.

For the last 5 ms, all the simulations from Star CCM+ exhibited the liquid penetration within the lower limits of experimental data, but for the OpenFOAM the values were over-predicted. This behavior have been seen in other literature as well (Lucchini et al., 2005).

Qualitative analysis of spray images

The Figure 7 shows an image obtained by the spray experiments in a time of approximately 1.4 ms.

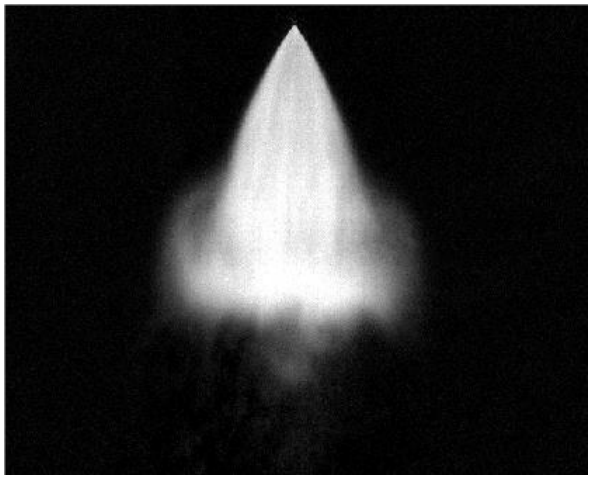

Figure 9: Image of experimental data (Guzzo, 2015)

In order to compare the OpenFOAM models with the experimental data, the spray was plotted at the time of 1.4ms at the plane perpendicular to the direction of the injection as seen in Fig. 10 and one for the Star CCM+ models at the same time, as seen in Fig. 11.

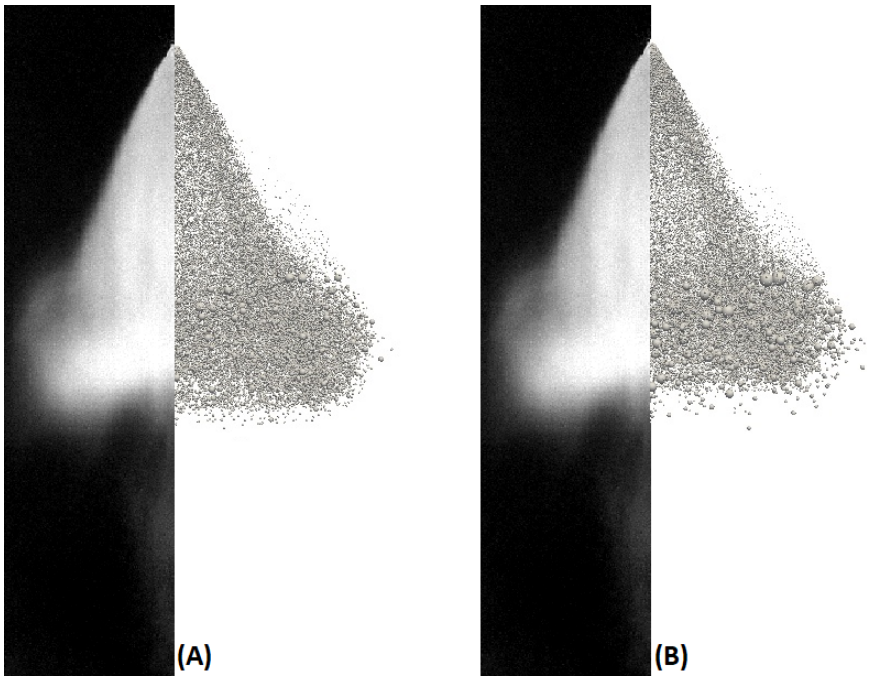

Figure 10: OpenFOAM: (A) - Images of Reitz Diwakat model / (B) - Images KHRT

The KHRT model simulations have higher number of smaller parcels. This is due the model KHRT promote the break-up of the particles and thus generate new particles, and new parcels. On the other hand, the model Reitz-Diwakar model only promotes a reduction in the size of existing particles when it undergoes the break-up phenomenon. In addition, it is possible to highlight that all simulations present the formation of the vortex in the front region of the spray.

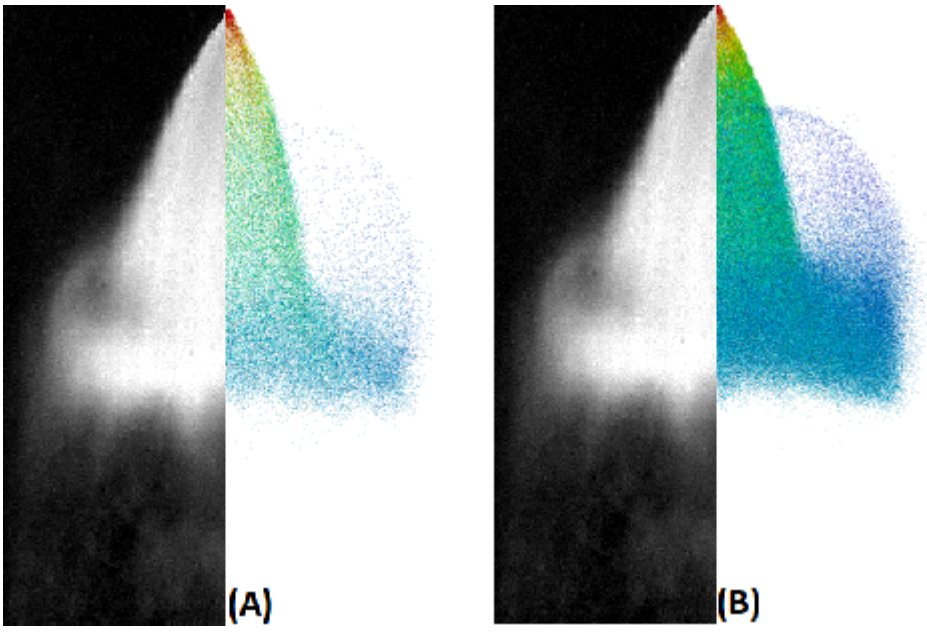

Figure 11: Star CCM +: (A) - Images of Reitz Diwakat model / (B) - Images KHRT

It is also possible to view the formation of the vortex in the experiment (Fig. 9). It comes primarily from aerodynamic forces of drag that tend to slow down the particles. Thus, for the

four models to the border regions parcels have lower speeds.

For the secondary break-up model Reitz-Diwakar (Fig. 10A and Fig. 11A), both software features acceptable results to the shape of the spray.

SMD- Sauter Mean Diameter

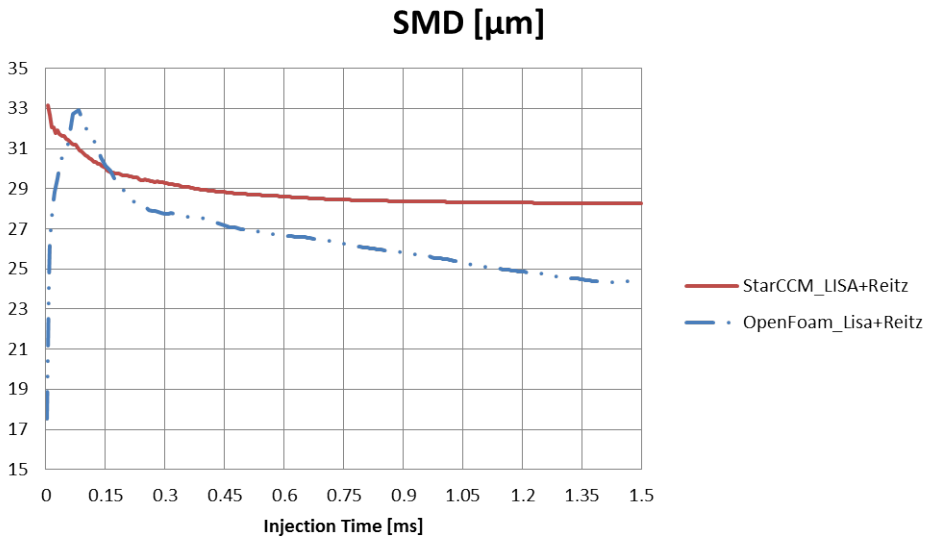

Figure 12: Sauter Mean Diameter - Model with LISA and Reitz Diwakar

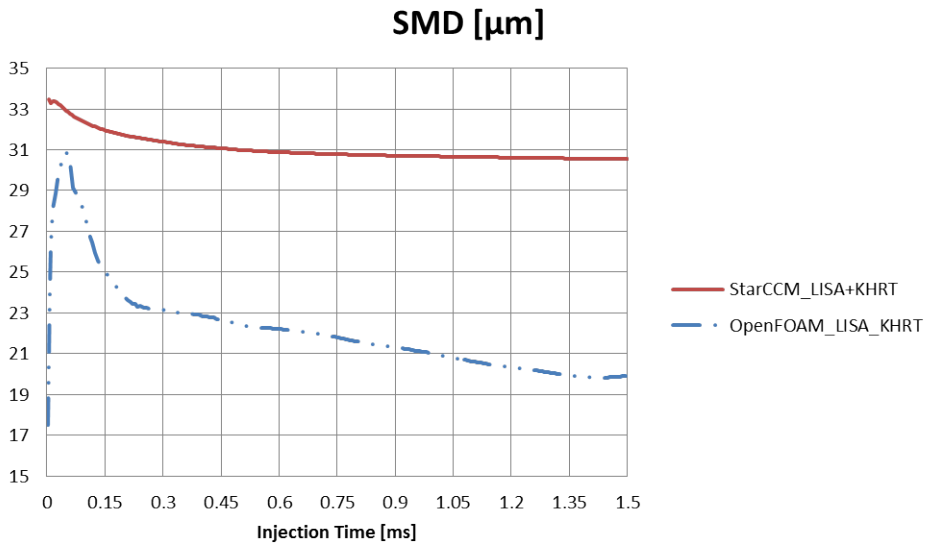

Figure 13: Sauter Mean Diameter - Model with LISA and KHRT

The size of the numerical domain and the mass injected per time step could differ from the simulations and it can affect the diameter of the parcels. The results shown in Fig. 12 and Fig. 13 present that the OpenFOAM simulations did get a better agreement with the literature (Huang and Lipatnikov, 2004), as there is a tendency in the increase of the SMD during the first

stages of the injection, this is due the increase of the injection velocity during the early stages of the injection. Then one a quasi-steady-state condition is reached near the injector nozzle, an increase in droplet size is observed (Tonini et al., 2009). Finally due to the break-up of the droplets the value from the SMD decreases.

2.5 Conclusions

Both software demonstrated good capabilities in the simulation of the penetration of the spray. However, Star CCM+ did achieve better correlation regarding the penetration as observed in Fig. 6 and Fig. 7. As for the qualitatively stand point the OpenFOAM did a better job representing the form of the spray, as seen in Fig. 10.

The results from OpenFOAM better resembles the literature data from SMD. And both simulations, S3 and S4, emulate the same tendencies as observed in Fig. 12 and Fig. 13. For further works it is necessary to measure SMD values in order to be able to completely correlate the numerical spray with the experimental data.

Even though Star CCM+ achieved better penetration results it is important to note that OpenFOAM is a free software. And as an open source software it is still possible to modify the numerical model to accurately achieve the necessary correlations with the experimental data.

ACKNOWLEDGEMENTS

Thanks to the laboratory Centro de Tecnologia da Mobilidade (CTM) of UFMG where all research activities, numerical and experimental, were performed leading to this article.

REFERENCES

C. Baumgarten. *Mixture formation in internal combustion engines*. 2006.

R. Bellman, R., Pennington. *Effects of surface tension and viscosity on Taylor instability*. PhD thesis, 1953.

CD-ADAPCO. Star-ccm+ version 9.02: User guide, 2014.

DieselNet. Emission standards - brazil: Light-duty vehicles. https://www.dieselnet.com/standards/br/ld.php, 2017.

M. E. e. a. Guzzo. Experimental Characterization of Ethanol Sprays from a Single Hole Direct Injection Injector. *SAE International*, 2015.

C. Huang. *Numerical Modelling of Fuel Injection and Stratified Turbulent Combustion in a Direct-Injection Spark-Ignition Engine Using an Open Source Code*. PhD thesis, 2014.

C. Huang and A. Lipatnikov. Modelling of Hollow-Cone Gasoline and Ethanol Sprays Using OpenFOAM 2 . Spray Models Implemented into the Standard OpenFOAM. *SAE International*, 2004.

C. Huang and A. Lipatnikov. Modelling of Gasoline and Ethanol Hollow-Cone Sprays Using OpenFOAM. *SAE Paper*, 2011.

D. Kah, S. V. Mittal, and H. Pitsch. LES of spray and combustion in an internal combustion engine. *Center for Turbulence Research*, pages 43–54, 2012.

F. S. Lee. Spray simulations with OpenFOAM. volume 35, pages 45–62. 2008.

A. H. Lefebvre. *Atomization and Sprays.*, volume 45. 1989.

T. Lucchini, G. D. Errico, and N. Nordin. CFD Modelling of Gasoline Sprays. *SAE Technical Paper*, 2005-24-08, 2005.

S. H. Park, H. J. Kim, H. K. Suh, and C. S. Lee. Atomization and spray characteristics of bioethanol and bioethanol blended gasoline fuel injected through a direct injection gasoline injector. *International Journal of Heat and Fluid Flow*, 30:1183–1192, 2009.

Y. S. Shim, G. M. Choi, and D. J. Kim. Numerical and experimental study on hollow-cone fuel spray of highpressure swirl injector under high ambient pressure condition. *Journal of Mechanical Science and Technology*, 22:320–329, 2008.

S. Tonini, M. Gavaises, and A. Theodorakakos. The role of droplet fragmentation in high-pressure evaporating diesel sprays. *International Journal of Thermal Sciences*, 48:554–572, 2009.